DALTON
FULL PAPER

Structure and reactivity of polymer-supported carbonylation catalysts †

Anthony Haynes,*[a] Peter M. Maitlis,[a] Ruhksana Quyoum,[a] Claire Pulling,[a] Harry Adams,[a] Sharon E. Spey[a] and Richard W. Strange[b]

[a] *Department of Chemistry, University of Sheffield, Brook Hill, UK S3 7HF. E-mail: a.haynes@sheffield.ac.uk*
[b] *Synchrotron Radiation Department, Daresbury Laboratory, Daresbury, Warrington, UK WA4 4AD*

Received 14th January 2002, Accepted 28th March 2002
First published as an Advance Article on the web 9th May 2002

The structure and reactivity of anionic complexes $[M(CO)_2I_2]^-$, supported on ion exchange resins based on quaternised poly(4-vinylpyridine-*co*-styrene-*co*-divinylbenzene) have been investigated using a variety of techniques. Infrared spectroscopy and EXAFS measurements show that the supported complexes adopt square planar structures very similar to those found in solution. The geometrical data obtained by EXFAS are also compared with new X-ray structures of the model compounds, $[4\text{-}RC_5H_4NMe][Rh(CO)_2I_2]$ (R = H (**1**) or Et (**2**)). The reactivity towards MeI of $[M(CO)_2I_2]^-$ supported on thin polymer films was probed directly *in situ* by IR spectroscopy. For M = Rh, oxidative addition of MeI was followed by rapid migratory CO insertion to give $[Rh(CO)(COMe)I_3]^-$, whereas for M = Ir oxidative addition gave a stable methyl complex, $[Ir(CO)_2I_3Me]^-$, mirroring the established solution chemistry. The reactions were first order in both [complex] and [MeI] and the observed pseudo-first order rate constants were comparable with those in homogeneous solution, although some subtle cation effects were observed. The kinetic measurements appear to be the first examples of quantitative rate data for fundamental reaction steps of a heterogenised transition metal catalyst.

Introduction

The use of transition metal catalysts dissolved in a liquid reaction medium is a feature of many commercial processes. One of the best known and most important examples is the manufacture of acetic acid from methanol and carbon monoxide. The "Monsanto process" developed in the late 1960s, uses a rhodium catalyst with an iodide promoter to produce acetic acid with very high selectivity (>99% based on MeOH).[1–3] This rhodium-based technology became the predominant method for manufacture of acetic acid, and was eventually acquired by BP Chemicals in 1986. Despite the great success of the Monsanto process, efforts to find an improved catalyst for methanol carbonylation have continued. The most significant breakthrough in recent times has been the introduction by BP Chemicals of the *Cativa*™ process in 1995, which utilises a homogeneous promoted iridium catalyst that gives even higher activity and selectivity than rhodium.[4] An important additional requirement for all homogeneous processes, however, is that the dissolved catalyst must be separated from the liquid product and recycled to the reactor without significant catalyst loss. A major goal of catalytic chemists is to immobilise (or "heterogenise") the homogeneous catalyst on a solid support in order to confine the catalyst to the reactor and overcome the need for a separate catalyst recycle step.

Immobilised carbonylation catalysts

A number of types of solid support have been employed to heterogenise rhodium catalysts for methanol carbonylation. These were reviewed[2] by Howard *et al.* in 1993 and include activated carbon, inorganic oxides, zeolites and a range of polymeric materials. One frequent approach to catalyst immobilisation is covalent attachment, in which the support (*e.g.* carbon or polystyrene) is modified to contain a pendant group (usually a phosphine) capable of acting as a ligand for the metal complex.[5] However, the susceptibility of covalently bound systems to metal–ligand bond cleavage makes irreversible leaching of the catalyst from the solid support a serious problem. This is particularly the case for methanol carbonylation, as pendant phosphines are prone to degradation by the aqueous acidic medium and quaternisation by methyl iodide.

This paper is concerned with an alternative strategy for catalyst immobilisation, using ion-pair interactions between ionic catalyst complexes and polymeric ion exchange resins. Mechanistic studies of the rhodium carbonylation catalyst, in particular by Forster and co-workers at Monsanto,[1] and more recently by the Sheffield group,[3,6] have given a detailed understanding of the catalytic cycle, depicted in Scheme 1. All four rhodium complexes in this cycle are anionic, which makes this system an attractive candidate for ionic attachment. This was first considered in 1980 by Drago *et al.*, who published results describing the effective immobilisation of the rhodium catalyst on polymeric supports based on methylated polyvinylpyridines.[7] The activity was reported to be equal to the homogeneous system at 120 °C with minimal leaching of the supported catalyst. The ionically bound complex $[Rh(CO)_2I_2]^-$ was identified by infrared spectroscopic analysis of the impregnated resin, indicating the presence of the same active species as found in the homogeneous process.

There has recently been a resurgence of interest in the ionic attachment strategy for catalytic methanol carbonylation, both from academic groups[8–10] and industry.[11] Most significantly, in 1998 Chiyoda and UOP announced their *Acetica*™ process,

† Electronic supplementary information (ESI) available: rotatable 3-D crystal structure diagrams in CHIME format, ORTEP plots of **1** and **2**, and tables of observed pseudo-first order rate constants for oxidative addition of MeI to $[Rh(CO)_2I_2]^-$ and $[Ir(CO)_2I_2]^-$ with polymeric and monomeric counter ions in CH_2Cl_2 or (for M = Rh) neat MeI. See http://www.rsc.org/suppdata/dt/b2/b200606e/

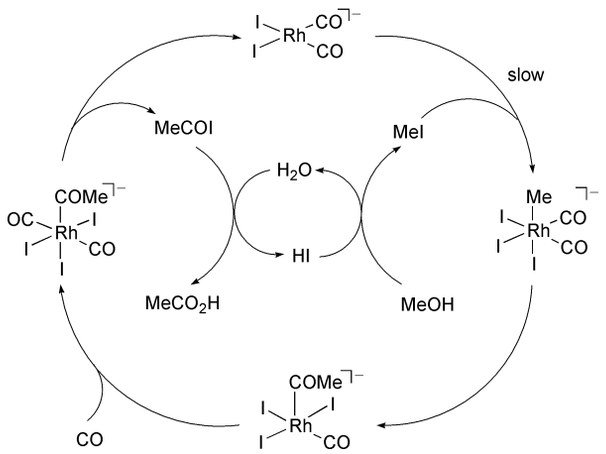

Scheme 1 Cycle for rhodium/iodide catalysed methanol carbonylation.

which uses a polyvinylpyridine resin tolerant of elevated temperatures and pressures.[12] The process, as reported, claims increased catalyst loading in the reactor (due to removal of solubility constraints of the homogeneous system) and reduced by-product formation as a consequence of lower water concentration. Ionic attachment of metal complexes to polymeric supports has also been employed for other catalytic processes, for example hydroformylation [13,14] and hydrogenation.[14,15]

This paper addresses the fundamental nature of the active catalytic species in ionically supported systems and reports some of the first kinetic data for individual reaction steps of such supported species. Although Drago's early studies identified the presence of supported $[Rh(CO)_2I_2]^-$ by IR, no further structural or mechanistic results were reported. As part of a collaborative project we have probed both the structure and the reactivity of polymer-supported $[Rh(CO)_2I_2]^-$, together with its Ir analogue. EXAFS was used to obtain structural information for the supported complexes and quantitative reactivity data were obtained using thin-film polymers (as opposed to beads) suitable for *in-situ* IR spectroscopy. We have shown that the same organometallic steps of the homogeneous catalytic carbonylation cycle illustrated in Scheme 1 also occur under mild conditions in the supported system. This has, for the first time, allowed kinetic measurements to be made on a fundamental reaction step of a heterogenised catalyst, enabling the behaviour of the polymer-supported and homogeneous catalysts to be compared in detail. It is demonstrated that the reactivity of $[M(CO)_2I_2]^-$ supported on an ion exchange resin is similar to the well-established solution chemistry.

Results and discussion

Preparation and characterisation of polymer-supported $[M(CO)_2I_2]^-$ (M = Rh, Ir)

The solid supports used in this study were macroporous co-polymers of 4-vinylpyridine and styrene crosslinked with divinylbenzene (Scheme 2). Polymers of this type in the form of beads (size: *ca.* 18–50 mesh) are available commercially (*e.g.* Reillex™ 425) and similar samples were also prepared for this study by Purolite.

For spectroscopic studies of supported metal complexes, a more convenient sample morphology was required and thin-film polymers‡ of similar stoichiometry to the beads were synthesised by the group of Sherrington at the University of Strathclyde. Full details of the methods used to prepare thin film polymers have been reported elsewhere.[16] Polymers were

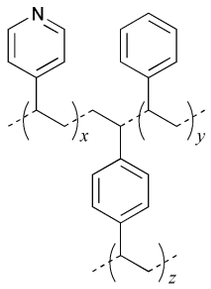

Scheme 2 Simplified representation of the structure of poly(4-vinylpyridine-*co*-styrene-*co*-divinylbenzene).

employed which had a range of 4-vinylpyridine content, thickness and degree of cross-linking (see Experimental for details). Macroporosity was introduced by carrying out the polymerisation in the presence of a porogen (*e.g.* 2-ethylhexan-1-ol or dodecanol). To generate the ion exchange resin, the pyridyl functionalities of the polymer were quaternised with an alkyl (generally methyl) iodide (Scheme 3).

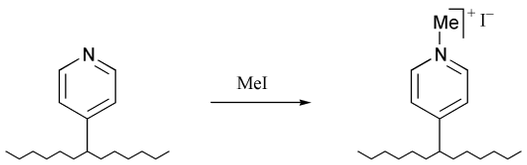

Scheme 3 Quaternisation of polymer pyridyl groups.

The rhodium complex was loaded onto the quaternised polymer support by the reaction with the dimeric precursor $[Rh(CO)_2I]_2$ dissolved in hexane (Scheme 4). The resulting

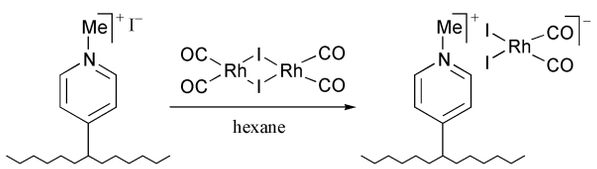

Scheme 4 Loading of $[Rh(CO)_2I_2]^-$ onto the polymer support.

polymer beads or films showed the characteristic yellow colour of $[Rh(CO)_2I_2]^-$. An infrared spectrum of the powdered beads (KBr disk) showed two weak ν(CO) absorptions of similar intensity at 2056 and 1984 cm^{-1}, consistent with the presence of the *cis*-dicarbonyl complex, $[Rh(CO)_2I_2]^-$ (2059, 1988 cm^{-1} in CH_2Cl_2) as reported by Drago *et al.*[7] and De Blasio *et al.*[10] Spectra of a much higher quality and intensity were obtained from polymer films loaded with rhodium complex, which displayed ν(CO) bands at 2056 and 1985 cm^{-1}, again confirming the presence of $[Rh(CO)_2I_2]^-$.

A different synthetic approach was required to load the corresponding iridium complex onto the polymer since the iridium analogue of $[Rh(CO)_2I]_2$ is not available. Therefore, instead of reacting a *neutral* precursor complex with the polymer-bound I^- to generate the desired anion, we employed the pre-formed *anionic* complex, $[Ir(CO)_2I_2]^-$ in an ion-exchange reaction (Scheme 5). Using this method, the liquid phase did

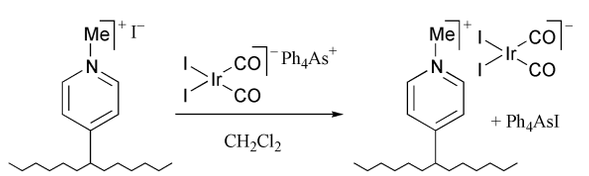

Scheme 5 Loading of $[Ir(CO)_2I_2]^-$ onto the polymer support.

not become completely colourless, indicating that a small amount of the Ir complex remained in solution at equilibrium The soluble salts (Ph_4AsI and $Ph_4As[Ir(CO)_2I_2]$) remaining

‡ Thin film polymers were previously employed by Jarrell and Gates (ref. 5) for *in situ* IR monitoring of a Rh catalyst covalently attached *via* pendant PPh_2 groups to a polystyrene support during vapour phase methanol carbonylation.

Table 1 Coordination parameters of polymer-supported $[M(CO)_2I_2]^-$ derived from EXAFS measurements[a]

Atoms	*r*/Å (M = Rh)	Debye–Waller/Å^2	*r*/Å (M = Ir)	Debye–Waller/Å^2	*r*/Å (soln) (M = Rh) [17]
2 C	1.84	0.006	1.86	0.025	1.845(4)
2 I	2.67	0.005	2.68	0.003	2.645(1)
2 O	3.00	0.005	3.02	0.009	2.961(2)

[a] Fit index 1.29 (Rh) and 1.07 (Ir); *R*-factor 38.1% (Rh) and 43.6% (Ir).

after the loading procedure were removed by washing the polymer with CH_2Cl_2. The infrared spectra (ν(CO) 2046 and 1968 cm^{-1} for both polymer beads and films) indicated the presence of the desired polymer-bound complex, $[Ir(CO)_2I_2]^-$.

Analysis of the loaded polymers (beads or films) by inductively coupled plasma optical emission spectrometry (ICP–OES) showed the metal contents to be 0.56–0.66% (Rh) and 0.79–0.86% (Ir) by weight. These values are in line with the observation that virtually all the metal complex is taken up from solution under the conditions of these loading experiments, and that 15–20% of the pyridinium sites are loaded with metal in the products.

Structural characterisation of polymer-supported complexes using EXAFS

The structures of the supported complexes described above were probed using rhodium and iridium extended X-ray absorption fine structure (EXAFS) measurements. The results of the curve-fitting analysis of the EXAFS traces for supported $[M(CO)_2I_2]^-$ are illustrated in Fig. 1. The Rh K-edge EXAFS

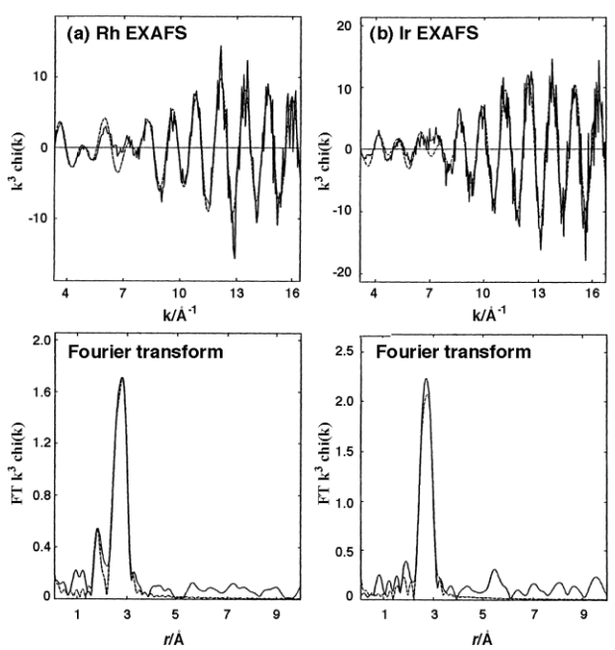

Fig. 1 EXAFS and Fourier transforms for polymer-supported $[M(CO)_2I_2]^-$ (M = (a) Rh, (b) Ir). Dotted lines show the theoretical fits to the experimental data.

shows very strong oscillations extending more than 1000 eV above the Rh absorption edge energy. The first (weaker) Fourier transform peak at *ca.* 1.8 Å corresponds to the carbons of the CO ligands. The peak at *ca.* 2.7 Å is associated with the heavy iodine atoms. Multiple scattering from the CO ligands also contributes to this peak, at about 3 Å. The basic simulation (dashed line Fig. 1a) using two iodide and two CO ligands almost completely accounts for the EXAFS data with the geometric information and fit parameters given in Table 1.

The EXAFS analysis for polymer-supported $[Ir(CO)_2I_2]^-$ (Fig. 1b) shows similar characteristics to the Rh system, with an intense peak at *ca.* 2.7 Å. This peak and the corresponding EXAFS amplitude is larger than for the Rh sample, causing the peak due to the C shell to appear smaller. The data are again well-simulated using two iodides and two carbonyl ligands with the geometric parameters given in Table 1. The scattering amplitudes of the more distant shells of atoms are weak making it very difficult to assign these peaks with confidence. However, for both metals there are features between the first and second peaks in the Fourier transforms which suggest the presence of additional scattering atom(s). Only light atoms such as nitrogen or oxygen are possible candidates, due to the short distance to Rh. A single additional nitrogen atom at a distance of 2.11 Å (Rh) or 2.10 Å (Ir) gave small improvements in the fits. However, the short distance to Rh is not compatible with a nitrogen atom from a pyridinium unit of the polymeric counter ion; attempts to fit this nitrogen to longer distances did not improve the simulation. An alternative explanation could be the presence of some residual water molecules which interact with the rhodium centre. However, there is no other evidence that $[M(CO)_2I_2]^-$ binds solvent ligands in the vacant axial coordination sites and these features in the EXAFS data may be artefacts. EXAFS measurements have been reported previously by Cruise and Evans for $Ph_4P[Rh(CO)_2I_2]$, dissolved in methanol.[17] Their geometric data, given in the final column of Table 1, are very similar to those for the polymer-supported complex, suggesting that ion pairing with a polymer support does not significantly perturb the structure of $[Rh(CO)_2I_2]^-$.

X-Ray crystal structures for $[4\text{-}RC_5H_4NMe][Rh(CO)_2I_2]$ (R = H, Et)

Rather surprisingly, there is no literature report of a crystal structure for the carbonylation catalyst, $[Rh(CO)_2I_2]^-$. Previous attempts in our laboratory to characterise salts of this anion crystallographically have been frustrated by disorder in the solid state. During the present study we synthesised the model compounds, $[4\text{-}RC_5H_4NMe][Rh(CO)_2I_2]$ (R = H (**1**) and Et (**2**)) as structural mimics of the polymer-supported system. These salts crystallised from CH_2Cl_2–Et_2O as deep yellow blocks suitable for X-ray diffraction studies. The stacking pattern of anions and cations for **1** is illustrated in Fig. 2 and single ion

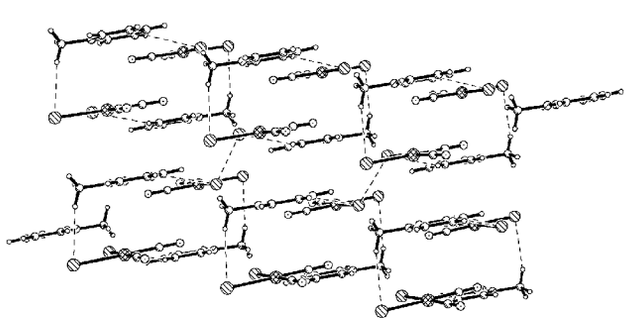

Fig. 2 X-Ray crystal structure of $[C_5H_5NMe][Rh(CO)_2I_2]$ (**1**) showing the layered stacking pattern of ions.

pairs are shown in Fig. 3 for both **1** and **2**. Geometrical data are compared with the EXAFS data in Table 2.

For both salts, the coordination geometry around rhodium is square planar with the two carbonyls *cis*, consistent with the infrared spectroscopic data. The Rh–C and Rh–I bond lengths

Table 2 Geometrical parameters (bond lengths in Å, angles in °) from X-Ray crystal structures of [4-RC_5H_4NMe][$Rh(CO)_2I_2$] (R = H (**1**) or Et (**2**)) and comparison with experimental EXAFS data and results of DFT computational studies on $[Rh(CO)_2I_2]^-$

	X-Ray (**1**)	X-Ray (**2**)	EXAFS (polymer)	EXAFS (soln)[17]	DFT[18]	DFT[19]
Rh–I	2.6539(12)	2.6623(8)	2.67(0.5)	2.645(1)	2.759	2.775
	2.6606(8)	2.6667(8)				
Rh–C	1.846(5)	1.845(7)	1.84(0.6)	1.845(4)	1.853	1.853
	1.864(5)	1.850(6)				
C–O	1.126(7)	1.129(8)	1.16[a]	1.12[b]	1.185	1.164
	1.132(7)	1.136(7)				
Rh ⋯ N (cation)	3.657(3)	3.853(5)				
Rh ⋯ ring centroid	3.81	4.03				
I–Rh–I	92.63(3)	94.94(2)			94.6	95.8
C–Rh–C	93.4(2)	92.9(3)			95.1	96.0
I–Rh–C	87.78(17)	85.46(18)			85.1	84.1
	86.18(16)	86.67(19)				
Rh–C–O	179.2(5)	179.6(6)		177(3)	178.2	177.5
	178.8(5)	178.7(6)				

[a] Assumes linear Rh–C–O. [b] Calculated from data in ref. 17.

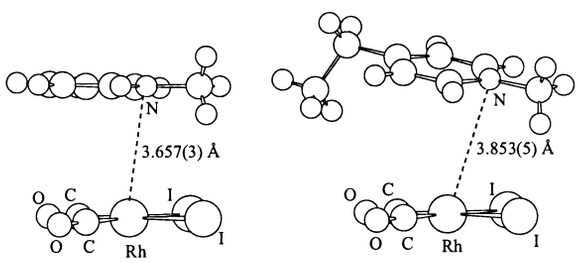

Fig. 3 Single ion pairs from the X-ray crystal structures of [4-RC_5H_4NMe][$Rh(CO)_2I_2$] (R = H (**1**), left and Et (**2**), right).

agree closely with those obtained by EXAFS for $[Rh(CO)_2I_2]^-$ in solution and supported on a polymer. The X-ray and EXAFS structures also provide a comparison with the results of recent computational studies on $[Rh(CO)_2I_2]^-$ using density functional theory (DFT).[18,19] The calculated geometrical parameters (Table 2) slightly overestimate the observed Rh–I and C–O distances but otherwise show good agreement with experiment.

The packing of ions in the lattice structures of these salts also shows some interesting features. For **1** the $[Rh(CO)_2I_2]^-$ anions and *N*-methylpyridinium cations are stacked in an alternating fashion with their planes almost parallel to each other (angle between planes *ca.* 4°). In **2**, the presence of the 4-ethyl substituent on the *N*-methylpyridinium cation forces the cation to twist away from a parallel ion-pair interaction with the rhodium complex (angle between planes *ca.* 15°) and this is reflected by somewhat longer Rh–N and Rh–ring centroid distances (Table 2). One could speculate that a similar arrangement of cation and anion might also exist for polymer-supported $[Rh(CO)_2I_2]^-$. In both X-ray structures the non-bonded Rh ⋯ N distances are much longer than the "fifth ligand" suggested by EXAFS analysis of the polymer-supported complex.

Reactions of polymer-bound $[M(CO)_2I_2]^-$

Although Drago *et al.*[7] used IR spectroscopy to show that the supported complex in their study was $[Rh(CO)_2I_2]^-$, and that under certain conditions conversion into $[Rh(CO)I_5]^{2-}$ could occur, no further investigations of the stoichiometric reactions of this supported complex were undertaken. We have carried out both qualitative and quantitative measurements on the reactivity of polymer-supported $[M(CO)_2I_2]^-$.

Reaction with methyl iodide

It is known that in solution, for M = Rh, the stoichiometric reaction with MeI leads to the acetyl complex $[Rh(CO)(COMe)I_3]^-$ *via* oxidative addition followed by rapid migratory CO insertion. The acetyl product exists as an iodide bridged dimer in the solid state[20] and as a solvated monomer in coordinating solvents.[21] In contrast, for M = Ir, oxidative addition is much faster and a stable methyl complex, $[Ir(CO)_2I_3Me]^-$, results as no spontaneous methyl migration occurs under ambient conditions.[22]

When a polymer film loaded with $[Rh(CO)_2I_2]^-$ was treated with excess methyl iodide (neat or diluted in CH_2Cl_2) the film changed colour from yellow to red–brown, similar to the colour change observed for the analogous reaction in solution. An IR spectrum of the resulting film showed a terminal ν(CO) band at 2053 cm^{-1} and a broad absorption around 1700 cm^{-1} for the acetyl carbonyl, similar to solution spectra of $[Rh(CO)(COMe)I_3]_n^{n-}$. The spectroscopic data do not indicate whether the polymer-bound product is monomeric or dimeric. When a dry polymer film containing the Rh acetyl complex was treated with gaseous carbon monoxide, very slow conversion into a product with infrared bands at 2074 and 1700 cm^{-1} was observed, consistent with the *trans*-dicarbonyl complex $[Rh(CO)_2(COMe)I_3]^-$ found in solution studies.[21] This carbonylation step was much faster if the CO was bubbled through a solvent (*e.g.* CH_2Cl_2) in which the polymer film was immersed, suggesting that molecules of CO enter the pores of the polymer much more efficiently when dissolved in a solvent. If left over several hours, the dicarbonyl acetyl species decomposed slowly to give $[Rh(CO)_2I_2]^-$, presumably *via* reductive elimination of acetyl iodide. Thus the same organometallic steps of the homogeneous catalytic carbonylation cycle illustrated in Scheme 1 also occur under mild conditions in the supported system. Similarly, reaction of polymer-supported $[Ir(CO)_2I_2]^-$ with methyl iodide gave the expected iridium–methyl product, $[Ir(CO)_2I_3Me]^-$ with ν(CO) bands at 2098 and 2046 cm^{-1}. These results demonstrate that the reactivity of $[M(CO)_2I_2]^-$ supported on an ion exchange resin is qualitatively similar to the well-established solution chemistry.

Leaching of metal complex from the polymer support

For the experiments described above, no metal species were detected by infrared or ICP analysis of the liquid phases (comprising MeI and CH_2Cl_2), indicating that the complexes remained bound to the polymer, with no measurable leaching into solution under these conditions. However, when polymer films loaded with $[Rh(CO)_2I_2]^-$ were immersed in coordinating solvents (*e.g.* MeCN), slow bleaching of the polymer and colouration of the liquid phase provided evidence for leaching of rhodium species into solution. IR spectroscopy indicated the presence of neutral solvated Rh complexes (*e.g.* $[Rh(CO)_2(NCMe)I]$, ν(CO) 2088 2024 cm^{-1}) in solution. Thus, leaching

occurs due to displacement of an iodide ligand from the Rh centre by solvent, generating a neutral complex which is no longer ionically bound to the polymer (Scheme 6a). Leaching could also be induced into CH_2Cl_2 by reaction with salts such as Bu_4NI (added in excess) leading to a simple ion exchange reaction (Scheme 6b).

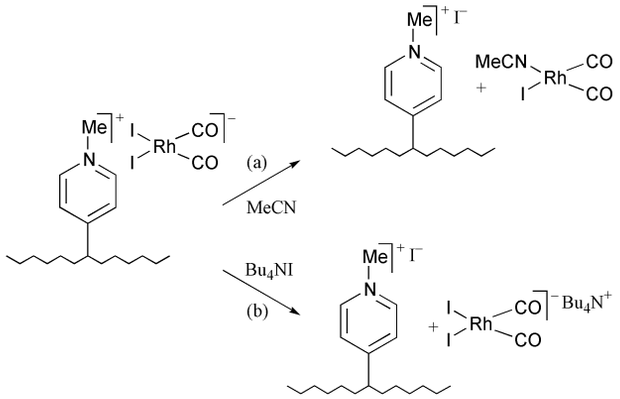

Scheme 6 Leaching of Rh species by (a) ligand substitution and (b) ion exchange.

Kinetic studies of MeI oxidative addition to polymer-supported $[M(CO)_2I_2]^-$

To extend the comparison between homogeneous and supported systems, we have carried out kinetic measurements on the reactions of polymer-supported $[M(CO)_2I_2]^-$ complexes with MeI. In order to monitor the reactions *in situ*, polymer films were inserted between the windows of a conventional infrared liquid cell, fitted with a thermostatted jacket. The cell was then filled with neat MeI or a solution of MeI in CH_2Cl_2, and transmission spectra recorded directly through the polymer film immersed in the MeI solution. An example of a series of spectra recorded in this way is shown in Fig. 4. The absorption

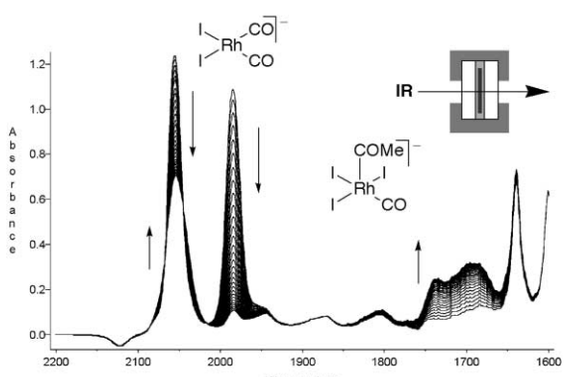

Fig. 4 Series of IR spectra for the reaction of neat MeI with $[Rh(CO)_2I_2]^-$ supported on a polymer film (25 °C). The arrangement of the cell is shown inset top right.

bands of $[Rh(CO)_2I_2]^-$ are replaced cleanly by those of the product acetyl complex, $[Rh(CO)(COMe)I_3]^-$, with the high frequency band of the reactant almost coinciding with the terminal ν(CO) band of the product.

A plot of absorbance *vs*. time for the low frequency reactant band at 1984 cm^{-1} (Fig. 5a) is well fitted by an exponential decay curve, showing that the reaction is first order in the concentration of $[Rh(CO)_2I_2]^-$. Pseudo-first order rate constants, k_{obs}, were obtained in this manner from a series of reactions at different methyl iodide concentrations. Fig. 5b shows that k_{obs} has a first order dependence on [MeI], and hence the reaction is second order overall, as in homogeneous solution. Changing the polymer morphology was found to have little effect on the kinetics of MeI oxidative addition to $[Rh(CO)_2I_2]^-$. Thus, sim-

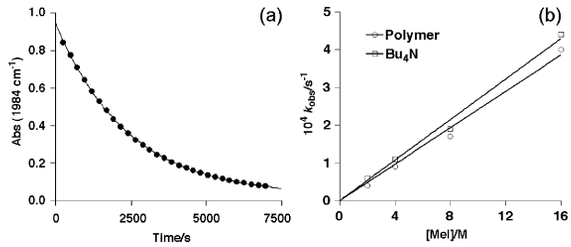

Fig. 5 (a) Decay of IR absorption at 1984 cm^{-1} with exponential curve fit (b) plots of k_{obs} *vs*. [MeI] for oxidative addition reactions of [Polymer][$Rh(CO)_2I_2$] and $Bu_4N[Rh(CO)_2I_2]$ (25 °C).

ilar rate constants (k_{obs} 4.2 (± 0.6) × 10^{-4} s^{-1} in neat MeI) were measured, for polymers with different degrees of cross-linking, 4-vinylpyridine content and thickness. Likewise, the use of polymers quaternised using propyl or *tert*-butyl iodide (rather than methyl iodide) had no significant effect upon the oxidative addition rate.

An apparent second order rate constant, k_2, for the reaction of polymer-supported $[Rh(CO)_2I_2]^-$ can be obtained from the slope of the plot of k_{obs} *vs*. [MeI] in Fig. 5b. The value of k_2 obtained in this way (2.57 × 10^{-5} M^{-1} s^{-1}, 25 °C) is very similar to that measured in parallel experiments for $Bu_4N[Rh(CO)_2I_2]$ in solution (2.71 × 10^{-5} M^{-1} s^{-1} in CH_2Cl_2). The corresponding k_{obs} values for the homogeneous reaction are also plotted in Fig. 5b for comparison. Care, however, must be taken in comparing second order rate constants in homogeneous and heterogeneous systems, since the effective concentration of a liquid reactant within the pores of a polymer may differ from that in the bulk solution.[23] In this case, therefore, $[MeI]_{polymer}$ is not necessarily the same as $[MeI]_{sol}$. Depending on whether MeI is preferentially concentrated or depleted in the polymer relative to the liquid phase, the real value of k_2 for the polymer-supported system may be higher or lower than that obtained by the classical method. Nevertheless, it is clear that k_{obs} for a given $[MeI]_{sol}$ is not markedly different for the supported complex and the Bu_4N^+ salt. In agreement with our model studies, De Blasio *et al.* have recently estimated that the rate constant for methanol carbonylation using polyvinylpyrrolidone-supported $[Rh(CO)_2I_2]^-$ differs from that for the homogeneous reaction by only a factor of *ca.* 2.[9]

A previous study[24] on the solution reactivity of $[Rh(CO)_2I_2]^-$ salts indicated that cation effects were small, but none of the cations tested in that study contained a pyridyl group. Therefore, in order to provide a closer mimic of the environment within the polymer, we have measured reaction kinetics for salts of $[Rh(CO)_2I_2]^-$ with cations of the type $[4\text{-}RC_5H_4NMe]^+$ (where R = H, Et, Bz). Interestingly, the pseudo-first order rate constants obtained in neat MeI for these reactions (listed in Table 3) are approximately double those obtained for either the Bu_4N^+ salt or the polymer-supported complex. Variable temperature studies were also carried out and Eyring plots of the resulting data gave the activation parameters listed in Table 3. Values of $\Delta H^{\ddagger}$ and $\Delta S^{\ddagger}$ are similar for all the cations tested and are typical for the oxidative addition reaction. The large negative entropy of activation found in each case is consistent with an initial S_N2 attack by the complex on MeI.[25] In view of the significant error bars, the faster reactions of the pyridyl salts cannot be ascribed with confidence to an enthalpic or entropic effect.

Kinetic measurements were also made for the reaction of MeI with polymer-supported $[Ir(CO)_2I_2]^-$. Under pseudo-first order conditions (0.08 to 0.32 M MeI in CH_2Cl_2), the decay of the 1946 cm^{-1} IR band due to $[Ir(CO)_2I_2]^-$ was well-fitted by an exponential decay curve, and a plot of the resulting k_{obs} values *vs*. [MeI] was linear, indicating a first order dependence on MeI. In this case, the rate constants were found to be consistently lower (by a factor of *ca.* 3) than those measured for the homogeneous reaction of $Ph_4As[Ir(CO)_2I_2]$. The activation

Table 3 Observed pseudo-first order rate constants (25 °C) and activation parameters for oxidative addition of MeI to $[M(CO)_2I_2]^-$

	Cation	$10^4\ k_{obs}{}^b/s^{-1}$	$\Delta H^‡$/kJ mol^{-1}	$\Delta S^‡$/J mol^{-1} K^{-1}
M = Rh	Polymer$^{+\,a}$	4.0	61 ± 4	−126 ± 15
	Bu_4N^+	4.4	54 ± 2	−151 ± 5
	$C_5H_5NMe^+$	7.1	58 ± 4	−133 ± 10
	4-$EtC_5H_4NMe^+$	9.2	53 ± 3	−149 ± 8
	4-$BzC_5H_4NMe^+$	7.9	55 ± 3	−142 ± 8
M = Ir	Polymer$^{+\,a}$	3.1	60 ± 2	−98 ± 5
	Ph_4As^+	10.3	53 ± 2	−112 ± 4

^{a} 11% Crosslinking, 4-vinylpyridine content 2 mmol g^{-1}, film thickness 96 μm. ^{b} Measured in neat MeI (concentration of 16 M) for M = Rh, and in 0.32 M MeI for M = Ir.

parameters derived from variable temperature data suggest that the lower rates result from a larger $\Delta H^‡$ which is only partially compensated for by less negative $\Delta S^‡$. The small net change (<3 kJ mol^{-1}) in $\Delta G^‡$ between the supported and homogeneous systems indicates that rather subtle effects are in operation, and the precise nature of these effects at the molecular level is unclear.

Conclusions

Spectroscopic and EXAFS studies show that the structure of $[Rh(CO)_2I_2]^-$ ionically bound to polyvinylpyridine-based resins is essentially identical to that found in solution and in the solid state (based upon two new crystal structures of salts of $[Rh(CO)_2I_2]^-$ containing *N*-methylpyridinium cations). Reactivity studies show that supported $[M(CO)_2I_2]^-$ complexes undergo oxidative addition with MeI in a similar fashion to the homogeneous reactions, yielding an acetyl complex (after rapid migratory insertion) for M = Rh and a stable methyl complex for M = Ir. Second order kinetics are observed for MeI oxidative addition to both metals, as found in solution. Observed rate constants for the reaction of supported $[Rh(CO)_2I_2]^-$ are very similar to those found for $Bu_4N[Rh(CO)_2I_2]$ in solution but *ca.* half those for salts containing monomeric *N*-methylpyridinium cations. For supported $[Ir(CO)_2I_2]^-$, rate constants were lower by a factor of *ca*. 3 than found for $Ph_4As[Ir(CO)_2I_2]$ in solution Whilst subtle cation effects on rate were observed, the close similarity in kinetic behaviour for homogeneous and heterogeneous reactions suggest that the permeability of the macroporous polymer to MeI is high, and that the reaction rate is not mass-transfer limited. The results demonstrate that the same sequence of organometallic reactions occur for the polymer-supported Rh catalyst as already established for the homogeneous system. The kinetic measurements provide the first example, to our knowledge, of quantitative rate data for fundamental reaction steps of heterogenised transition metal catalysts.

Experimental

Materials and synthetic methods

Solvents and reagents were purified by standard methods.[26] Dichloromethane and acetonitrile were distilled from calcium hydride after reflux; methyl iodide was distilled from calcium hydride and stored under nitrogen, over mercury in a foil wrapped vessel; diethyl ether was distilled from a purple solution of sodium/benzophenone immediately before use. Other reagents were used as supplied: Ph_4AsCl, Bu_4NI, (Aldrich), rhodium and iridium chloride hydrates (Johnson Matthey). Standard Schlenk techniques and glassware were used for preparative reactions.[27] Nitrogen and carbon monoxide (BOC CP Grade) were dried through a short (20 × 3 cm diameter) column of molecular sieve (4A) which was regularly regenerated; the carbon monoxide was also passed through a short column of activated charcoal to remove any iron pentacarbonyl impurity.[28]

Metal complexes $[Rh(CO)_2I]_2$,[24] $Bu_4N[Rh(CO)_2I_2]$[24] and $Ph_4As[Ir(CO)_2I_2]$[22] were prepared by established methods. Poly(4-vinylpyridine-*co*-styrene-*co*-divinylbenzene) was supplied in the form of beads (Reillex™ 425 and similar samples made by Purolite) or prepared as thin films (dimensions *ca.* 76 × 14 mm × 43–96 μm) at the University of Strathclyde. Full details of the preparation and characterisation of the thin-film polymers have been reported elsewhere.[16] In our studies, films were used with a range of 4-vinylpyridine content (0.5–8.7 mmol g^{-1}, and degree of crosslinking (11 or 22% divinylbenzene).

Quaternisation of polymers

Quaternisation of the pyridine groups of the polymer was carried out by slow addition of the polymer beads (typically 1 g) or films to ethanol (40 cm^3), to which was added methyl iodide (2 cm^3, excess). The mixture was heated to 50 °C for 2 h and then cooled. The quaternised polymer was washed with ethanol followed by acetone and then dried *in vacuo*.

Loading of $[M(CO)_2I_2]^-$ onto polymer supports

For M = Rh the quaternised polymer (1 g) was added to a solution of $[Rh(CO)_2I]_2$ (15 mg, 26 μmol) in hexane (20 cm^3) and stirred for 4 h (until the solution in contact with the polymer beads or films became colourless). The polymer beads or films were filtered and washed with hexane, dried *in vacuo* and stored under an atmosphere of CO at −10 °C. The loaded polymers were characterised by IR spectroscopy (ν(CO)/cm^{-1}: 2056, 1984) and by ICP–OES (wt % Rh determined as 0.56 (Reillex 425 beads), 0.59 (Purolite eads) and 0.66 (thin film)). For M = Ir a similar procedure was employed, contacting the polymer with a solution of $Ph_4As[Ir(CO)_2I_2]$ (23 mg, 26 μmol) in CH_2Cl_2 (20 cm^3). The loaded polymers were characterised by IR spectroscopy (ν(CO)/cm^{-1}: 2046, 1968) and by ICP–OES (wt % Ir determined as 0.81 (Reillex 425 beads), 0.79 (Purolite beads) and 0.86 (thin film)).

Preparation of $[4\text{-}RC_5H_4NMe][Rh(CO)_2I_2]$ (R = H, Et, Bz)

The *N*-methylpyridinium salts $[4\text{-}RC_5H_4NMe][Rh(CO)_2I_2]$ were prepared in a similar procedure to the Bu_4N^+ salt, by reaction of the appropriate *N*-methylpyridinium iodide with $[Rh(CO)_2I]_2$. Recrystallisation from CH_2Cl_2–diethyl ether mixtures afforded $[4\text{-}RC_5H_4NMe][Rh(CO)_2I_2]$ as yellow solids which were dried *in vacuo* and stored under an atmosphere of CO at −10 °C. Crystals of $[C_5H_5NMe][Rh(CO)_2I_2]$ (**1**) and [4-$EtC_5H_4NMe][Rh(CO)_2I_2]$ (**2**) suitable for X-diffraction were obtained by slow diffusion of diethyl ether into a CH_2Cl_2 solution of the compound at 0 °C. Crystals of **2** were found to melt on warming to room temperature, whereas those of **1** remained solid. Elemental analysis for **1** (%) C 19.2, H 1.58, N 2.67; expected for $C_8H_8NI_2O_2Rh$: C 18.9, H 1.58, N 2.76.

Instrumentation

Infrared spectra were recorded using either a Nicolet Magna 560 FTIR spectrometer operated by OMNIC software or a

Mattson Genesis FTIR spectrometer using WINFIRST software. Solution spectra were measured using a liquid cell with CaF_2 windows (pathlength 0.1 or 0.5 mm). Elemental analyses (CHN) were performed by the University of Sheffield microanalysis service using a Perkin-Elmer 2400 Elemental Analyser. Precious metal analyses were determined (at Johnson Matthey) by ICP–OES using a Thermo Jarrell Ash Polyscan 61E instrument with the following general method. Sample vials were weighed out then washed with Aristar grade acetic acid into 250 cm^3 beakers. The vials were then dried in an oven, allowed to cool and then reweighed. The solvents present in the samples were gently evaporated off to leave a gum at the bottom of each flask. Aristar grade nitric acid (20 cm^3) was then added and the temperature of the hotplate increased so that wet oxidation occurred. Any fine residue from this process was filtered off through a 0.2 micron filter, dry oxidised in a furnace at 700 °C and fused with sodium peroxide (1 g). The resultant flux was leached with Aristar grade hydrochloric acid (5 cm^3) and this solution combined with the filtrate from above and made up to a total volume of 100 cm^3. This was then diluted tenfold and analysed against suitable standards by ICP–OES, using ruthenium as an internal standard at a concentration of 100 ppb in all samples, blanks and standards.

Kinetic measurements

The reactions of polymer-supported $[Rh(CO)_2I_2]^-$ with methyl iodide were monitored using FTIR spectroscopy in a solution cell (CaF_2 windows, 0.5 mm path length) fitted with a thermostatted jacket. A strip of the metal loaded polymer film was placed between the CaF_2 plates and the cell reassembled. Methyl iodide (neat or diluted to known concentration with CH_2Cl_2) was added to the cell which was then placed in the sample compartment of the spectrometer. Infrared spectra (ratioed against a solvent background recorded prior to the kinetic run) were recorded at programmed time intervals and stored electronically. Data sets of absorbance against time for the frequencies of interest were extracted from the stored spectra. The pseudo-first-order-rate constants were obtained by fitting exponential decay curves to the experimental data using Kaleidagraph software.

EXAFS measurements

EXAFS data (Rh K-edge ((23220 eV) or Ir L_{III}-edge (13419 eV)) were collected in transmission mode on station 9.2 of the Daresbury Synchrotron Radiation Source, operating at 2 GeV with an average current of 150 mA. A water-cooled Si(220) double crystal monochromator was used, with its angle calibrated by running an edge scan of a 5 μm Rh or Ir foil. For each sample 4 scans were recorded at room temperature from 200 eV below the absorption edge to 1200 eV (16 $Å^{-1}$) above; count time used k^3 weighting; spectra analysed using EXCURV97[29] employing the fast curved wave approximation.[30] Multiple scattering from the CO ligands was simulated using a linear geometry for the M–C–O units.

X-Ray crystallography

For both structures, data collected were measured on a Bruker Smart CCD area detector with Oxford Cryosystems low temperature system. Hydrogen atoms were placed geometrically and refined with a riding model (including torsional freedom for methyl groups) and with U_{iso} constrained to be 1.2 (1.5 for methyl groups) times U_{eq} of the carrier atom. Complex scattering factors were taken from the program package SHELXTL[31] as implemented on the Viglen Pentium computer.

$[C_5H_5NMe][Rh(CO)_2I_2]$ (1). Crystal data for $C_8H_8I_2O_2Rh$; M = 506.86; yellow blocks were formed by slow diffusion of diethyl ether into a dichloromethane solution of the compound at 5 °C; crystal dimensions 0.35 × 0.30 × 0.20 mm. Triclinic, a = 7.137(2), b = 7.503(3), c = 12.697(3) Å, α = 78.932(18)° β = 87.860(17)° γ = 75.72(3)°, U = 646.6 (4) $Å^3$, Z = 2, D_c = 2.604 Mg m^{-3}, space group $P\bar{1}$ (C'_i, no. 2), Mo-Kα radiation (λ = 0.71073 Å), μ(Mo-Kα) = 6.073 cm^{-1}, F(000) = 460. Cell parameters were refined from the setting angles of 43 reflections (θ range 1.63 < 28.35°). Reflections were measured from a hemisphere of data collected of frames each covering 0.3 degrees in omega. Of the 4331 reflections measured, all of which were corrected for Lorentz and polarisation effects and for absorption (maximum and minimum transmission coefficients of 0.3764 and 0.2250) 2879 independent reflections exceeded the significance level $|F|/\sigma(|F|) > 4.0$ The structure was solved by direct methods and refined by full matrix least squares methods on F^2. Refinement converged at a final $R = 0.0309$ ($wR_2 = 0.0857$ for all 2977 unique data, 129 parameters, mean and maximum δ/σ 0.000, 0.001), with allowance for the thermal anisotropy of all non-hydrogen atoms. Minimum and maximum final electron density −1.309 and 0.827 e A^{-3}. A weighting scheme $w = 1/[\sigma^2(F_o^2) + (0.0347P)^2 + 1.78P]$ where $P = (F_o^2 + 2F_c^2)/3$ was used in the latter stages of refinement.

$[4\text{-}EtC_5H_4NMe][Rh(CO)_2I_2]$ (2). Crystal data for $C_{10}H_{12}I_2NO_2Rh$; M = 534.92; yellow blocks were formed by slow diffusion of diethyl ether into a dichloromethane solution of the compound at 5 °C; crystal dimensions 0.46 × 0.24 × 0.14 mm^3. Monoclinic, a = 9.127(2), b = 13.553(3), c = 12.251(3) Å, β 92.465(5)°, U = 1514.1(7) $Å^3$, Z = 4, D_c = 2.347 Mg m^{-3}, space group $P2_1/n$ (a non-standard setting of $P2_1/c$ C'_{2h} no. 14), Mo-Kα radiation (λ = 0.71073 Å), μ(Mo-Kα) = 5.193 mm^{-1}, F(000) = 984. Cell parameters were refined from the setting angles of 100 reflections (θ range 2.24 to 28.33°). Reflections were measured from a hemisphere of data collected of frames each covering 0.3 degrees in omega. Of the 8771 reflections measured, all of which were corrected for Lorentz and polarisation effects and for absorption by semi empirical methods based on symmetry-equivalent and repeated reflections (minimum and maximum transmission coefficients 0.1986 and 0.5301) 3034 independent reflections exceeded the significance level $|F|/\sigma(|F|) > 4.0$. The structure was solved by Patterson synthesis and refined by full matrix least squares methods on F^2. Refinement converged at a final $R = 0.0467$ ($wR_2 = 0.1178$, for all 3598 data, 145 parameters, mean and maximum δ/σ 0.000, 0.000), with allowance for the thermal anisotropy of all non-hydrogen atoms. Minimum and maximum final electron density −1.484 and 1.651 e $Å^{-3}$ (the latter 0.89 Å from I2). A weighting scheme $w = 1/[\sigma^2(F_o^2) + (0.0656P)^2 + 2.3183P]$ where $P = (F_o^2 + 2F_c^2)/3$ was used in the latter stages of refinement.

CCDC reference numbers 178080 and 178081.

See http://www.rsc.org/suppdata/dt/b2/b200606e/ for crystallographic data in CIF or other electronic format.

Acknowledgements

The research described in this paper was carried out as part of a DTI/EPSRC LINK project: "Polymer-supported carbonylation catalysts", Oct 1997–March 2000 involving BP Chemicals, Johnson Matthey, Purolite International and the Universities of Sheffield and Strathclyde, (grant ref. No. GR/L61149). We thank our co-workers on the project, Professor David Sherrington, Dr Paul Findlay and Dr Salla-M. Leinonen (University of Strathclyde) and Dr Jim Dale (Purolite UK, Pontyclun) for providing polymeric materials, Mr Simon Collard and Dr Andrew Chiffey (Johnson Matthey, Royston) for performing the ICP measurements and Mr Philip Howard, Dr Mike Simpson and Dr Mike Jones (BP Chemicals, Hull) for valuable discussions. We acknowledge the provision of time on DARTS, the UK national synchrotron radiation service at the CLRC Daresbury Laboratory, through funding by the EPSRC (DARTS reference 98E14).

References

1 T. W. Dekleva and D. Forster, *Adv. Catal.*, 1986, **34**, 81; D. Forster, *Adv. Organomet. Chem.*, 1979, **17**, 255.
2 M. J. Howard, M. D. Jones, M. S. Roberts and S. A. Taylor, *Catal. Today*, 1993, **18**, 325.
3 P. M. Maitlis, A. Haynes, G. J. Sunley and M. J. Howard, *J. Chem. Soc., Dalton Trans.*, 1996, 2187.
4 G. J. Sunley and D. J. Watson, *Catal. Today*, 2000, **58**, 293; M. J. Howard, G. J. Sunley, A. D. Poole, R. J. Watt and B. K. Sharma, *Stud. Surf. Sci. Catal.*, 1999, **121**, 61; J. H. Jones, *Platinum Met. Rev.*, 2000, **44**, 94.
5 M. S. Jarrell and B. C. Gates, *J. Catal.*, 1975, **40**, 255.
6 A. Haynes, B. E. Mann, G. E. Morris and P. M. Maitlis, *J. Am. Chem. Soc.*, 1993, **115**, 4093.
7 R. S. Drago, E. D. Nyberg, A. El A'mma and A. Zombeck, *Inorg. Chem.*, 1981, **3**, 641; R. S. Drago and A. El A'mma, *U.S. 4328125*, 1982.
8 D. Z. Jiang, X. B. Li and E. L. Wang, *Macromol. Symp.*, 1996, **105**, 161; R. J. Sowden, M. F. Sellin, N. De Blasio and D. J. Cole-Hamilton, *Chem. Commun.*, 1999, 2511.
9 N. De Blasio, M. R. Wright, T. E, C. Mazzocchia and D. J. Cole-Hamilton, *J. Organomet. Chem.*, 1998, **551**, 229.
10 N. De Blasio, T. E, A. Kaddouri, C. Mazzocchia and D. J. Cole-Hamilton, *J. Catal.*, 1998, **176**, 253.
11 C. R. Marston and G. L. Goe, *E.P. 0 277 824*, 1988; Y. Shiroto, K. Hamato, S. Asaoka and T. Maejima, *E.P. 0 567 331*, 1993; D. J. Watson, B. L. Williams and R. J. Watt, *E.P. 0 612 712*, 1994; M. O. Scates, R. J. Warner and G. P. Torrence, *U.S. 5466874*, 1995; T. Minami, K. Shimokawa, K. Hamato, Y. Shiroto and N. Yoneda, *U.S. 5364963*, 1994.
12 N. Yoneda, T. Minami, J. Weiszmann and B. Spehlmann, *Stud. Surf. Sci. Catal.*, 1999, **121**, 93.
13 N. Yoneda, Y. Nakagawa and T. Mimami, *Catal. Today*, 1997, **36**, 357; J. Balué and J. C. Bayón, *J. Mol. Catal. A: Chem.*, 1999, **137**, 193; L. Alvila, T. A. Pakkanen, T. T. Pakkanen and O. Krause, *J. Mol. Catal.*, 1992, **71**, 281; S. C. Tang, T. Paxson and L. Kim, *J. Mol. Catal.*, 1980, **9**, 313; M. E. Ford and J. E. Premecz, *J. Mol. Catal.*, 1983, **19**, 99; I. Guo, B. E. Hanson, I. Toth and M. E. Davis, *J. Mol. Catal.*, 1991, **70**, 363; I. Toth, B. E. Hanson, I. Guo and M. E. Davis, *Catal. Lett.*, 1991, **8**, 209; E. Schwab and S. Mecking, *Organometallics*, 2001, **20**, 5504.
14 R. T. Smith, R. K. Ungar, L. J. Sanderson and M. C. Baird, *Organometallics*, 1983, **2**, 1138.
15 M. Kralik, M. Hronek, V. Jorik, S. Lora, G. Plama, M. Zecca, A. Biffis and B. Corain, *J. Mol. Catal. A: Chem.*, 1995, **101**, 143; D. E. Bergbreiter, B. L. Case, Y.-S. Liu and J. W. Caraway, *Macromolecules*, 1998, **31**, 6053; E. Renaud and M. C. Baird, *J. Chem. Soc., Dalton Trans.*, 1992, 2905; I. Toth and B. E. Hanson, *J. Mol. Catal.*, 1992, **71**, 365; Y. Chauvin, D. Commereuc and F. Dawans, *Prog. Polym. Sci.*, 1977, **5**, 95.
16 D. C. Sherrington, *J. Assoc. Lab. Automation*, 2000, **5**, 75; D. C. Sherrington, *J. Mater. Chem.*, 2000, **10**, 2031.
17 N. A. Cruise and J. Evans, *J. Chem. Soc., Dalton Trans.*, 1995, 3089.
18 T. Kinnunen and K. Laasonen, *J. Mol. Struct. (Theochem)*, 2001, **540**, 91.
19 E. A. Ivanova, P. Gisdakis, V. A. Nasluzov, A. I. Rubailo and N. Rösch, *Organometallics*, 2001, **20**, 1161.
20 G. W. Adamson, J. J. Daly and D. Forster, *J. Organomet. Chem.*, 1974, **71**, C17.
21 H. Adams, N. A. Bailey, B. E. Mann, C. P. Manuel, C. M. Spencer and A. G. Kent, *J. Chem. Soc., Dalton Trans.*, 1988, 489.
22 P. R. Ellis, J. M. Pearson, A. Haynes, H. Adams, N. A. Bailey and P. M. Maitlis, *Organometallics*, 1994, **13**, 3215.
23 D. C. Sherrington, in *Polymer-supported Reactions in Organic Synthesis*, eds. D. C. Sherrington and P. Hodge, J. Wiley and Sons, Chichester, UK, 1980.
24 A. Fulford, C. E. Hickey and P. M. Maitlis, *J. Organomet. Chem.*, 1990, **398**, 311.
25 T. R. Griffin, D. B. Cook, A. Haynes, J. M. Pearson, D. Monti and G. E. Morris, *J. Am. Chem. Soc.*, 1996, **118**, 3029.
26 D. D. Perrin, W. L. F. Armerego and D. R. Perrin, *Purification of Laboratory Chemicals*, Pergamon Press, Oxford, 1988.
27 D. F. Shriver, *The Manipulation of Air Sensitive Compounds*, J. Wiley and Sons, New York, Chichester, 1986.
28 A. Haynes, P. R. Ellis, P. K. Byers and P. M. Maitlis, *Chem. Ber.*, 1992, **28**, 517.
29 SERC Daresbury Laboratory EXCURV92 program, N. Binsted, J. W. Campbell, S. J. Gurman and P. C. Stephenson, Daresbury, 1991.
30 P. A. Lee and J. B. Pendry, *Phys. Rev. B: Condens. Matter*, 1975, **11**, 2795; S. J. Gurman, N. Binsted and I. Ross, *J. Phys. C*, 1984, **17**, 143.
31 G. M. Sheldrick, in SHELXTL, An integrated system for solving and refining crystal structures from diffraction data (Revision 5.1), Bruker AXS LTD, Madison, WI, 1997.